Formamide Hydrolysis Investigated by Multiple-Steering ab Initio Molecular Dynamics

Michele Cascella, Simone Raugei, and Paolo Carloni*

International School for Advanced Studies and INFM−DEMOCRITOS Modeling Center for Research In Atomistic Simulation, Via Beirut 2-4, 34014 Trieste, Italy

Received: May 26, 2003; In Final Form: August 4, 2003

The first step of formamide hydrolysis in aqueous solution has been studied coupling ab initio molecular dynamics to the multiple-steering molecular dynamics approach. We have investigated the reaction at both neutral (water addition) and alkaline (hydroxyl ion addition) pH. The activation barrier of the water-addition reaction (44 kcal mol^{-1}) is much larger than that of the reaction catalyzed at alkaline pH (15 kcal mol^{-1}). The solvation shell structure of the hydroxyl anion plays an important role in the dynamical and energetic properties. In particular, the free-energy profile for the hydroxyl ion addition is completely solvent induced, and its transition state properties can be essentially related to the dynamics of the hydration shell of the hydroxyl ion.

1. Introduction

The cleavage of peptide bonds is a fundamental reaction catalyzed by a large number of different protease enzymes.[1] The investigation of model systems such as amides in aqueous solution is of interest as it is a reference for the enzyme-catalyzed reaction.[2]

Small amides are very stable in aqueous solution and hydrolysis of their amidic bond does not occur at room temperature and physiological pH;[3] in these conditions, the uncatalyzed reaction,

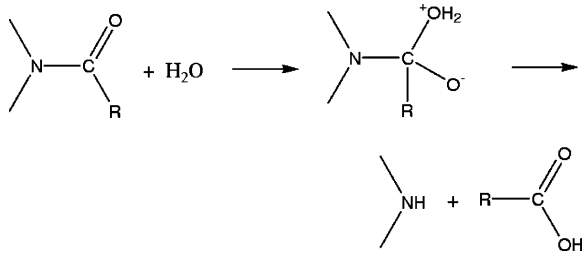

which is initiated by water addition, is so disadvantaged that, even though there is some experimental evidence for this reaction to occur,[3] kinetic data favor a base-catalyzed mechanism even at neutral pH.[3,4] On the other hand, both acidic and basic solutions exhibit catalytic activity on the reaction. From a biochemical point of view, the base-promoted reaction

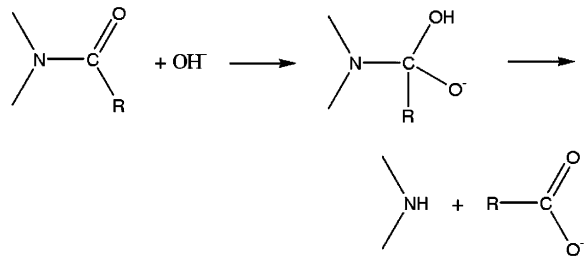

is more important than the acid-promoted one because of its closer analogy with most enzymatic mechanisms.[2] The experimental activation free energy for the base-catalyzed reactions is of ≈20−30 kcal mol^{-1},[5,6] depending on the substrate and the temperature.

The first step of the reaction at both neutral and alkaline pHs has been the subject of many computational studies. The ab initio calculated activation free energy of the uncatalyzed reaction is about 55 kcal mol^{-1} in vacuo[7,8] and 48−51 kcal mol^{-1} in the presence of the solvent,[9] whereas the free-energy barrier for the base-catalyzed reaction decreases to 18 kcal mol^{-1}. Furthermore, for the base-catalyzed reaction, the activation barrier has been shown to be completely solvent induced.[10−12] Empirical valence bond calculations by Warshel and coworkers[2,13,14] on the base-catalyzed reaction confirm this proposal.

In the reaction with water, the geometry of the reactants along the reaction pathway is similar to that in vacuo, and solvent effects are taken into account a posteriori.[7,8,9,15−23] This approximation may lead to an overstabilization of concerted mechanisms for the water addition, which lack significant charge separation, typical of reactions in aqueous environment.[2] In contrast, when water molecules are explicitly included,[9,22] the reaction mechanism depends on the number of the water molecules around the amide molecule. Furthermore, the transfer of a proton from the water molecule to the nitrogen atom occurs through a H-bond network along the water molecules in the cluster.

For the OH^- addition, solvent effects have been included using empirical potential fitted on gas-phase calculations[10,11] or implicit or dipolar solvation models,[2] which reproduce the reactants solvation energies.[24−27] The calculated activation free energy agrees well with the experimental values.[5,6] However, since the solvent is treated at a lower computational level than the reactants, the description of the dynamics of the solvent interacting with the reactants might not be well described. In this regard, it is important to note that the hydroxyl ion has nontrivial solvation structures,[28] which have been described by first principles molecular dynamics simulations.[29−33] These simulations have suggested the existence of two structures, triangular ($H_7O_4^-$) and squared-base pyramidal ($H_9O_5^-$), depending on OH^- concentration. These findings were able to rationalize experimental IR and Raman spectra of hydroxyl solutions.[34]

* Corresponding author. E-mail: carloni@sissa.it.

10.1021/jp035458c CCC: $27.50
Published on Web 12/05/2003

In this paper, we present an ab initio Car−Parrinello molecular dynamics (CPMD)[35] investigation of the initial step of the uncatalyzed and the base-catalyzed reactions of formamide in liquid water. A full first-principle quantum-mechanical approach with explicit inclusion of the solvent (treated at the same level of theory of the reactants) is expected to provide a quantitative understanding of the reaction mechanism without employing a priori assumptions. The calculation of the activation free energy has been done coupling standard CPMD to the fast-growth technique introduced by Jarzynski[36] into a multiple-steering molecular dynamics (MSMD) framework. The present study shows that when a suitable choice of the reaction coordinate can be made, the MSMD methodology, along with CPMD, enables efficient and accurate calculations of activation barriers. Our calculations indicate that solvent reorganization plays a crucial role in the OH^--attack reaction. Indeed, the desolvation mechanism of the OH^- is the origin of the solvent-induced activation barrier of the OH^- addition.

2. Computational Details

2.1. Free-Energy Calculations. Since bond breaking and forming require the crossing of a relatively large activation barrier, a method to sample the relevant reaction coordinate must be employed. Several sampling techniques of reaction paths in the condensed phase are available, see, e.g., refs 36−42.

In the present study, we have used the MSMD[36] approach, which establishes a relation between the nonequilibrium dynamics and equilibrium properties.[43−60] An experimental validation of the reliability of Jarzynski's methodology has also recently appeared.[61] Many articles and reviews treat in detail the theory we refer to.[36,62,63] In the following paragraphs, we will only recall the relevant concepts strictly necessary for the ensuing discussion.

Let $H(\mathbf{r},t)$ be the Hamiltonian of a system that is subject to an external time-dependent perturbation, and let $\Delta G(t')$ and $W(t')$ be, respectively, the change in free energy and the external work performed on the system as the system evolves from $t = 0$ to $t = t'$. Here $\mathbf{r}$ indicates a configuration of the whole system. According to Jarzynski,[36] $\Delta G(t')$ and $W(t')$ are related to each other by the following identity

$$e^{-\beta \Delta G(t')} = \langle e^{-\beta W(t')} \rangle \tag{1}$$

where the brackets represent an average taken over an ensemble of trajectories. The previous equality can be also reformulated as[63]

$$e^{-\beta[H(\mathbf{r}',t') - G(0)]} = \langle \delta(\mathbf{r}(t') - \mathbf{r}') e^{-\beta W(t')} \rangle. \tag{2}$$

The Hamiltonian $H(\mathbf{r},t)$ can be written as the sum of the time-independent Hamiltonian of the unperturbed system, $H_0(\mathbf{r})$, plus the time-dependent external potential. In the present study, as well as in refs 58−60 and 63, the perturbation has been chosen to be a harmonic potential, which minimum position moves at constant velocity υ according to

$$H(\mathbf{r},t) = H_0(\mathbf{r}) + \frac{k}{2}[z(\mathbf{r}) - z_0 - \upsilon t]^2 \tag{3}$$

where $z(\mathbf{r})$ represents a chosen reaction path. In this way, at any given time, only a small window around the equilibrium position $z(\mathbf{r}) = z_0 + \upsilon t$ is sampled. By substituting eq 3 into eq 2, one finds

$$G(z') = -\beta^{-1} \ln\langle \delta[z(\mathbf{r}(t')) - z'] e^{-\beta W(t')} \rangle \tag{4}$$

Thus, the free energy of a process along a selected reaction coordinate can be computed performing a representative number of finite time transformations, collecting at each time step the work done, and then properly averaging it.

Equation 4 requires the convergence of an exponential, which is slow. Thus, it is more convenient to use a second-order cumulant expansion[57]

$$G(z') \approx -\beta^{-1} \ln\langle \delta[z(\mathbf{r}(t')) - z'] \rangle + \langle W(t') \rangle_{z'} - \frac{\beta}{2} \sigma^2 \langle W(t') \rangle_{z'} \tag{5}$$

where $\langle \cdots \rangle_{z'}$ denotes an average restricted to trajectories satisfying the condition $z(\mathbf{r}(t')) = z'$ and σ^2 is the variance of the average work done.

2.2. Electronic Structures and CPMD Calculations. First-principles molecular-dynamics simulations have been carried out within the (CPMD)[35] approach, using the CPMD code.[65]

Our model for the reaction in water has been composed by a formamide molecule (FOR) and 56 water molecules enclosed in a periodic box of 13.5 Å × 11.8 Å × 11.8 Å edges (Figure 1). This corresponds to take explicitly into account two complete solvation shells of formamide plus a part of the third shell. The OH^- attack has been investigated in a simulation cell obtained from the previous one by mutating a randomly chosen water molecule into a hydroxyl ion (Figure 2). Here, a uniform positive background has been added to neutralize the total electric charge. In this way, it has been possible to simplify the model and avoid the continuous presence of the counterion near the reaction site, which could nonphysically alter the dynamics because of the small size of the cell. In this regard, we would like to point out that previous CPMD studies of charged aqueous solutions, carried out with simulation cells comparable to ours in size, number of atoms, and charge, showed that the finite-size effect is not crucial in determining the main dynamical properties of an ionic aqueous solution.[32,64]

CPMD employs density functional theory (DFT) for electronic structure calculations. In the present study, Becke[66] and Lee, Yang, and Parr[67] (BLYP) exchange and correlation functionals have been used. Norm-conserving Martins−Troullier pseudopotentials[68] have been employed to describe the interactions between the core and valence electrons for all atoms but hydrogens, for which a Von Bart−Car-type pseudopotential[69] has been used to smooth out the short-range Coulombic nuclear potential. The Kohn−Sham orbitals of valence electrons have been expanded in plane waves with kinetic energy up to 70 Ry. A fictitious electronic mass of 800 au has been used.[35] This choice has allowed integration of the equations of motion with a time step of 5 au (≈0.12 fs).

The electronic properties and dipole moments were analyzed by projecting our delocalized basis-set onto maximally localized Boys' Orbitals (BOs),[70,71] whose centers of charge can be directly associated to concepts such as chemical bonds and lone pairs.[72]

Three distinct simulations have been carried out as described in the following:

(i) Formamide in Water. CPMD (5.2 ps) have been carried out at room temperature, using a Nosé-Hoover chain of thermostats.[73−75] This simulation time turned out to be sufficient to converge the structural properties (radial and angular distribution functions) calculated in this work. The last configuration of this simulation has been used as the initial model of calculations (ii) and (iii).

(ii) Water Addition to FOR. One water molecule (WAT hereafter) has been randomly selected, and the distance between

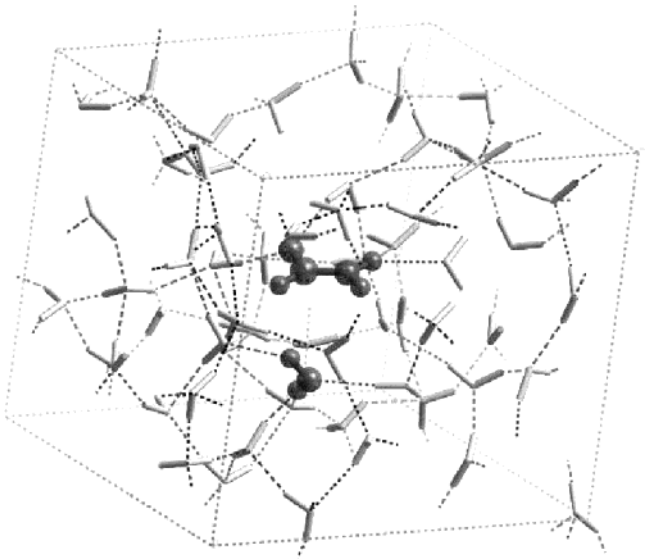

Figure 1. Simulation box for WAT addition to FOR. FOR and WAT are drawn in dark-gray balls and sticks, and the other water molecules are drawn in light-gray cylinders.

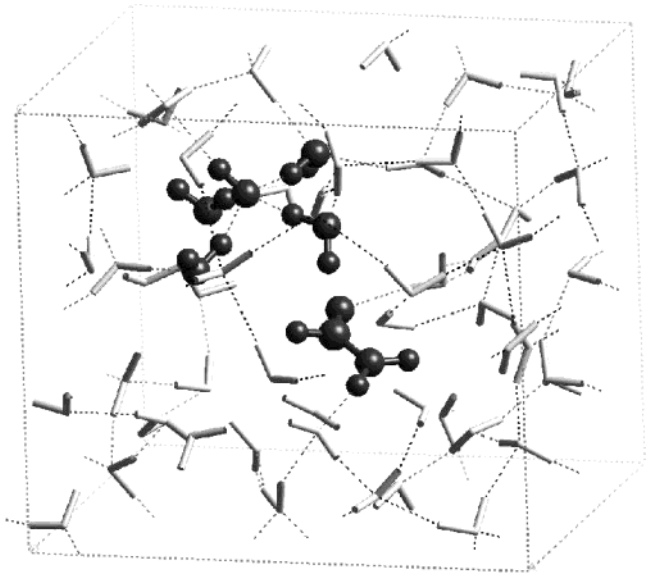

Figure 2. Simulation box for HYD addition to FOR. FOR, HYD, and its hydration shell are drawn in dark-gray balls and sticks, and the other water molecules are drawn in light-gray cylinders.

its oxygen atom (O_{WAT}) and the carbon atom (C) has been chosen as the reaction coordinate. The system was first equilibrated for 3.5 ps, applying a harmonic potential as defined in eq 3 to this coordinate. To choose the initial distance, two preliminary simulations have been performed. In these simulations, WAT was first restrained and then moved toward FOR from an initial distance of 5.0 and 3.5 Å, respectively, from C. Water molecules at these distances are structurally different. Only water molecules at 5.0 Å from C are similar to those in the bulk. In both cases, WAT has followed the same reactive path, suggesting that possible deviations from the reactive pathway, which are dependent on the relaxation distance, can be neglected. Thus, we have decided to relax our system by restraining the $C-O_{WAT}$ distance to around 3.5 Å, with a force constant $k = 50$ kcal mol^{-1} Å^{-2}.

Six configurations equispaced in time (500 fs) have been used as starting points for the MSMD runs. The reaction coordinate has been slowly decreased by shortening at constant speed $v = 1.1$ Å ps^{-1} the distance corresponding to the minimum of the restraining harmonic potential until formation of the adduct. The inverse reaction has been investigated by reversing the dragging velocity for two of the six simulations.

It has been previously shown[59] that the convergence of the free-energy profile does not depend on the harmonic force constant if the latter is of the same magnitude of the energy barrier to be crossed, that is in this case ≈50 kcal mol^{-1}.[9]

(iii) OH^- Addition to FOR. MSMD runs have been performed following the same protocol as for WAT addition. In this case, one of the two reagents brings a negative charge. Because of the long-range nature of electrostatic interactions between the two reagents, the oxygen atom of the hydroxyl ion (O_{HYD}) has been restrained at a longer distance from C (4.5 Å) by a harmonic potential with force constant $k = 25$ kcal mol^{-1} Å^{-2}. During the equilibration phase, a coordination constraint[76] has been set on O_{HYD} in order to avoid unwanted proton transfers. Six steering simulations have been carried out for both the direct and inverse processes, using as starting point configurations saved every 500 fs from the previous simulation.

2.3. Accuracy of the Quantum-Chemical Calculations. The majority of the studies of chemical reactivity carried out so far using DFT seem to indicate that the reaction barriers are underestimated (see, for example, refs 77 and 78). To have an estimate of a possible intrinsic error in our pseudopotential-DFT/BLYP calculations, we have computed the activation energy for the addition of water to formamide in vacuo (concerted mechanism). No zero-point-energy effects have been taken into account. The calculation has been performed at the DFT/BLYP level, as described in section 2.2, in a 8.5 Å × 9.0 Å × 9.0 Å cell. The value obtained (40.5 kcal mol^{-1}) is only slightly lower than the value reported by Jensen et al.[8] at the MP2/6-311G** level (42.8 kcal mol^{-1}). This result makes us confident that the present DFT/BLYP calculations are adequate to reasonably describe the energetics of the reactions investigated in water solution.

3. Results and Discussion

3.1. Dynamics of Formamide in Water. In water, FOR acts as a H-bond acceptor via its carbonyl oxygen (O_{FOR}). The integration of the first peak of the radial distribution function (RDF) between O_{FOR} and water's hydrogen atoms (H_w), reported in Figure 3a, shows that this group forms, on average, H-bonds with two water molecules. The maximum of the $O_{FOR}-H_w$ peak is located at about 1.8 Å, in agreement with previous reports.[79,80] FOR acts also as a H-bond donor via the two nitrogen hydrogens (H_N). These hydrogens exhibit a different affinity for water (Figure 3b); in fact, the trans hydrogen (H_t) is characterized by a maximum at the typical H-bond distance (≈1.8 Å) that is 0.5 units higher than that found for the cis hydrogen (H_c). The two peaks integrate to 0.9 and 0.7 oxygen atoms, respectively.

Water molecules H-bonded to the carbonyl have longer residence time than those interacting with H_N. Indeed, the height of the first minimum of the $O_{FOR}-H_w$ RDF is ≈0.2 (Figure 3a), whereas the values for the two H_N hydrogens are ≈0.3 and 0.4 for H_t and H_c, respectively (Figure 3b). This difference was also observed by Jorgensen and Swenson using empirical potentials;[79] although, in our full-quantum simulation, the difference is more pronounced. Furthermore, in the present study, the H-bond interaction of the carbonyl or the amidic group with the solvent is stronger or weaker, respectively, than that reported treating water with nonpolarizable empirical force fields.[79,80] Thus, our findings support the recent proposal, based

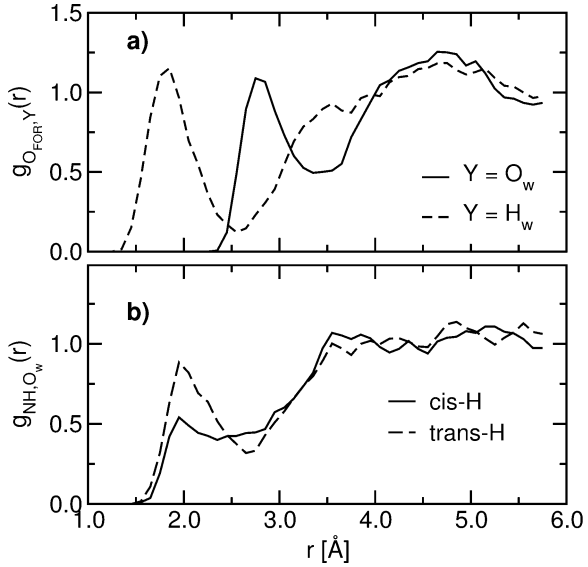

Figure 3. Radial distribution functions of FOR in water, $g(\mathbf{r})$. (a) $g(\mathbf{r})$ between the O_{FOR} atom and water's oxygens (solid line) and water's hydrogens (dashed line). (b) $g(\mathbf{r})$ between amidic cis (H_c, solid line) and trans (H_t, dashed line) hydrogens and solvent oxygens.

on nonlinear spectroscopy measurements[83] and previous simulations,[64,81,82] that polarization effects could play a determinant role for water exchange rates.

Structural fluctuations have been analyzed by monitoring two dihedral angles related to the C−N bonds:[80] (i) $\delta = {}^1/_2(\phi_1 + \phi_2)$, where ϕ_1 and ϕ_2 are the dihedral angles identified by the atoms $O_{FOR}-C-N-H_c$ and $O_{FOR}-C-N-H_t$, respectively. This angle measures the capability of the molecule to twist around the C−N bond. Its MD-averaged value ($\approx 90 \pm 7°$) evidences the average planar structure of this molecule, characterized by moderate fluctuations. (ii) $\omega = \phi_{H_c-N-C-H_t}$, which describes the out-of-plane rocking of H_t and H_c. Its average value ($180 \pm 22°$) also implies a planar equilibrium structure but with a relatively larger vibrational amplitude. The difference in fluctuations can be related to the electronic structure of the π C−N bond, herein described in terms of BOs.[70−72]

During the twisting motion, the BOs remain localized in the same region of the space, as no significant shift from its equilibrium positions has been observed. In fact, the π system spans over the C−O_{FOR} and C−N bonds (three-center π system), allowing only small distortions around the C−N bond. During the rocking motion, on the contrary, the BO's move longitudinally along the C−N bond. This shift corresponds to an enhancement of the sp^3 character of the N atom, as evidenced in Figure 4; in fact, upon structural distortion of the molecule, one BO migrates toward the N atom, while the other migrates between N and C atoms. This higher capability of the electronic structure to undergo modifications upon atomic motion leads to a relatively larger amplitude of this vibrational mode.

3.2. Hydrolysis Reaction via Ab Initio MSMD Calculations. The present study is one of the first applications of the MSMD technique to ab initio atomistic simulations. Therefore, it represents a benchmark test for this methodology. Particular attention has been paid to the convergence properties of the free-energy profile as a function of the number of trajectories and to possible hysteresis effects. The latter have been estimated by comparing the two profiles obtained for the direct and the reverse reaction. The free-energy profiles for each reaction have been obtained by simulating a total of about 10−12 ps.

3.2.1. Water Addition to FOR. *Energetics.* The free-energy profile of the direct addition of water to formamide converges

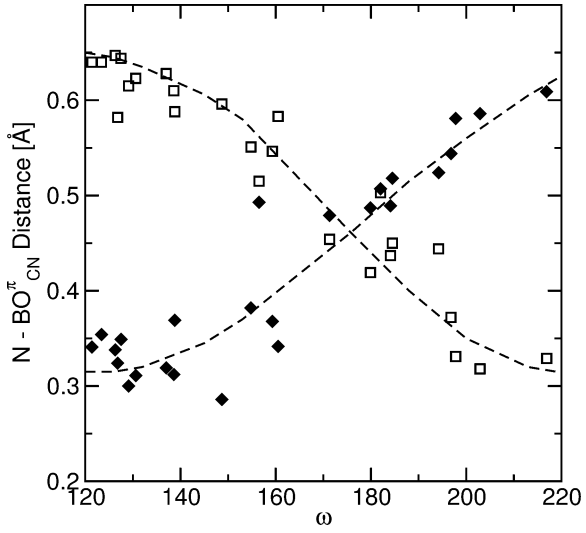

Figure 4. Displacement of the two BOs (empty and filled symbols) associated to the C−N bond as a function of the ω dihedral angle ($H_c-N_{FOR}-C_{FOR}-H_t$). The dashed lines are only a guide for the eye.

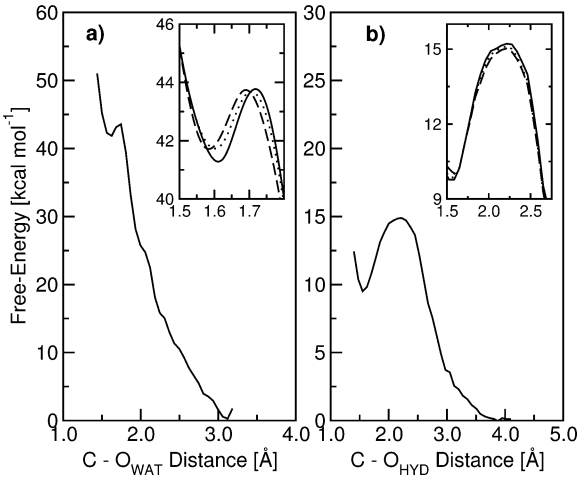

Figure 5. Free-energy profile of WAT (a) and HYD (b) addition to FOR. In the insets, the TS region is enlarged to show the convergence of the free energy as a function of the number of trajectories (two, dashed line; four, dotted line; six, solid line). In both simulations, no differences in the free-energy profiles obtained averaging over five and six trajectories have been evidenced.

within few steering trajectories (Figure 5a). Furthermore, within our statistical uncertainty, it coincides with that of the reverse reaction. Hence, for this system, hysteresis does not seem to be relevant. The calculated free energy of the reaction is of 44 kcal mol^{-1}, which is fairly good agreement with previous calculations.[9] The inverse reaction features a small activation energy (2 kcal mol^{-1}). Although this suggests that the intermediate is very labile, it must be pointed out that recent findings[84] indicate that the free energy of the intermediate in this reaction may be overestimated by the BLYP calculations by several kcal mol^{-1}.

Structural Features. At large WAT−FOR distances, the solvation of reactants resembles that in the bulk; in particular, the WAT hydrogen-bond length is $\approx 1.9 \pm 0.2$ Å, as in CPMD simulations of bulk water. WAT attacks FOR perpendicularly to the FOR molecular plane. The molecular planes of FOR and WAT atoms get almost parallel as the transition state (TS) is approached. Furthermore, as the reaction coordinate goes below 2.5 Å, one of the two H-bonds received by WAT breaks. After breaking, the new solvation structure of WAT is conserved up to the formation of the tetrahedral adduct (parts a and c of Figure

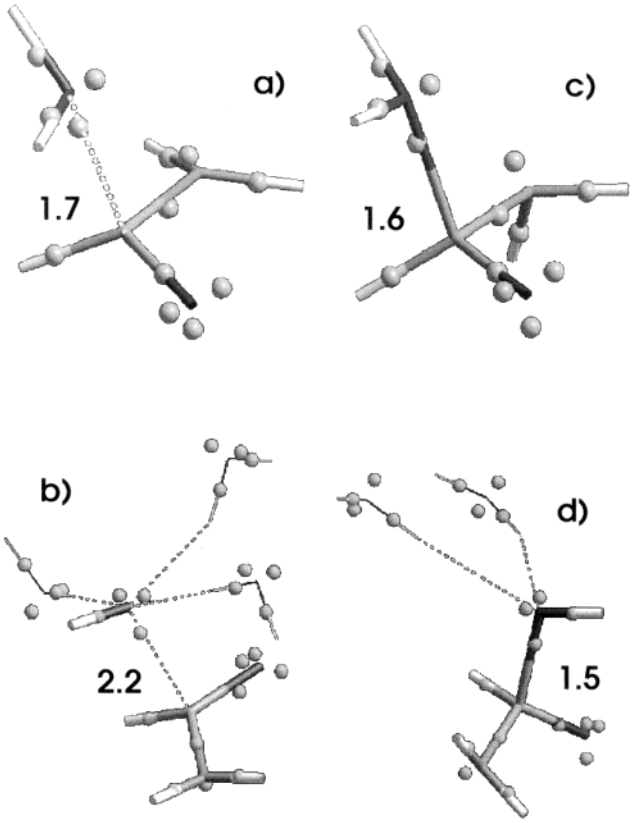

Figure 6. Structure of the transition state and the intermediate of WAT (a and c) and HYD addition (b and d). BOs are drawn as spheres. Water molecules H-bonded to OH^- are drawn as sticks. For the sake of clarity, the other water molecules are not drawn. The C−O distance (in Å) is also reported.

6). The two H-bonds donated by WAT never break during reaction. The tetrahedral angles of the TS depend on the structure of the solvent, without showing a preference for staggered or eclipsed configurations of the two molecules.

The approach of WAT to FOR, up to the TS, neither induces relevant changes in the solvation shell of FOR nor involves interactions between the reactants' solvation shells. Thus, the dynamical features of the direct reaction are essentially related to the approaching motion of the two reagents that do not require any complex rearrangement of the solvent close to the TS. The TS is found at a $C-O_{WAT}$ distance of 1.73 Å. The equilibrium distance of the intermediate is found at a distance of 1.61 Å. The intermediate adduct resembles the TS (late TS, Figure 6c). After formation of the tetrahedral intermediate, the N atom acts as the H-bond acceptor, whereas the carbonyl oxygen is able to coordinate three H-bonds.

Electronic Structures. The electronic structure does not change significantly until the TS is reached ($C-O_{WAT} = 1.73$ Å). Then, as the π system of FOR is disrupted, one of the two BOs[70−72] migrates close to the oxygen atom, and the other migrates between the two atoms of the carbonyl group, as evidenced in Figure 7a, where the relative displacement of the two BOs related to the CO bond is shown.

It is interesting to compare these results with those obtained in human caspase-3[85] and HIV-1 aspartic protease,[86] for which similar computational setups have been used. In the present study, during the water attack, the BOs related to O_{WAT} lone pairs remain localized around the oxygen atom until the reaction coordinate is as short as ≈2.0 Å (Figure 8a), when one of the two BOs migrates toward the C atom to form the σ bond. Indeed, until that distance, WAT is practically as polarized as

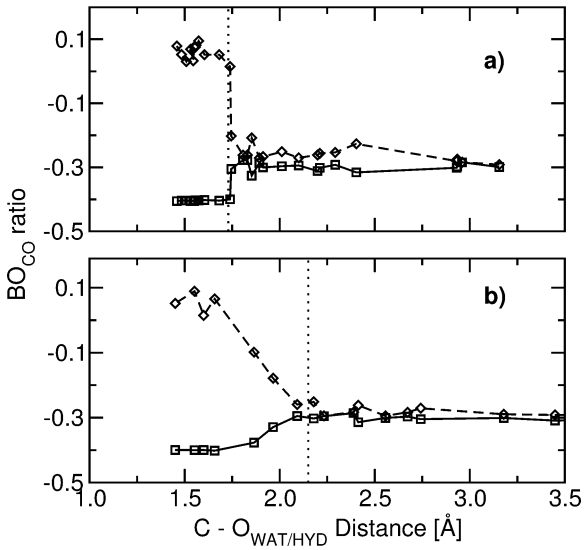

Figure 7. Relative displacement of the carbonyl BOs during WAT (a) and HYD (b) approach to FOR. The relative displacement is computed as $(d_{C-BO} - d_{C-O})/d_{C-O}$, where d_{C-O} is the $C_{FOR}-O_{FOR}$ bond length and d_{C-BO} is the $C_{FOR}-BO$ distance. The vertical dotted line indicates the position of the TS.

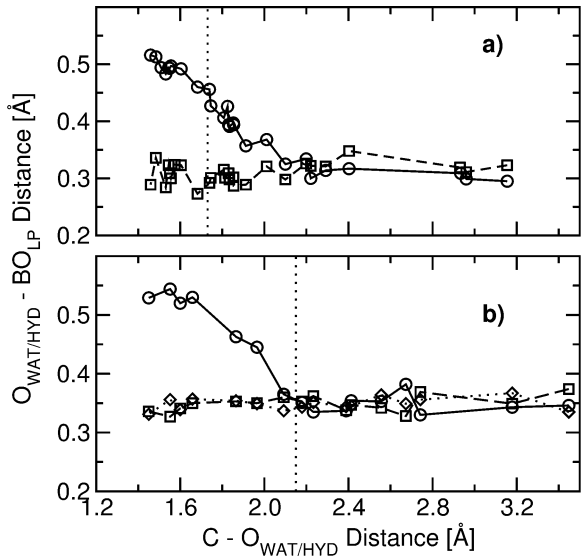

Figure 8. Displacement of BOs related to the lone pairs of WAT (a) and HYD (b) along the reaction coordinate. The vertical dotted line indicates the position of the TS.

in the bulk, showing a MD-averaged dipole moment of ≈3.1 D, that is slightly larger than that of the other water molecules in the cell (≈3.0 D). Similar values have been calculated, using DFT/BLYP, for peptide hydrolysis catalyzed by these enzymes. This suggests that polarization of the incoming water is not likely requested for the catalytic process. In these enzymatic systems, in contrast, the key factor for catalysis might be the presence of a proton-shuttle system, which is able to efficiently deprotonate the reactive water molecule. This is performed by a catalytic histidine (His237) in caspase-3,[85] whereas in HIV-1 protease it is the catalytic Asp dyad (Asp25, Asp25′).[86] In the present system, this efficient proton shuttle is absent, and both WAT hydrogen atoms remain bound to O_{WAT} until the tetrahedral adduct is formed. Only after this event are $O_{WAT}-H$ bonds weakened, and the average bond distance increases from 0.97 to 1.05 Å. Hence, deprotonation can happen only after the low-rate step of the reaction has occurred. This event has been observed in two out of six MSMD simulations.

3.2.2. OH^- Addition to FOR. The method here employed for computing free-energy profiles requires, as the standard thermodynamic integration, that all the possible (collective) coordinates can relax with respect to that chosen as the reaction coordinate. This is not the case for the *direct* reaction of the base-catalyzed attack, since the strongly H-bonded OH^- water molecules do not allow, on the time scale of our simulations, for the large rearrangements of the solvation shell that are deemed necessary for the reaction to occur. In other words, the approaching time of OH^- to FOR is too short compared to that required for the OH^- shell to undergo partial disruption.

In our simulation, OH^- has a 4-fold coordination, in agreement with previous calculations at a pH comparable to ours,[29−33] and it has to progressively lose two solvation waters to react to FOR. Both the four- and three-water solvation structures are very stable.[30] As a consequence, O_{HYD} cannot approach the C atom relaxing correctly with respect to the harmonic restraint; hence, the free energy cannot be reliably calculated with a finite number of trajectories. Simulations performed with a slower pulling speed ($\upsilon = 0.2$ Å ps^{-1}) have manifested the same problem. In contrast, the *inverse* reaction is not affected by this problem (Figure 5b). In fact, in this case there is a preorientation of the reactants (e.g., the $H_{HYD}-O_{HYD}-C$ angle) in the cleavage of the $C-O_{HYD}$ bond, and the subsequent hydration of OH^- occurs readily because the strong H-bond interactions between the hydroxyl ion and water molecules drive a fast formation of the solvation cluster. Hence, the free-energy profile of the inverse reaction can be calculated using the $C-O_{HYD}$ distance as reaction coordinate.

Energetics. For the reasons discussed above, here we will refer only to the free-energy profile of the inverse reaction. As for the uncatalyzed reaction, the free energy profile converges within a few trajectories (Figure 5b, inset). The calculated activation free energy with respect to solvent-separated FOR and OH^- is 15 kcal mol^{-1} (Figure 5b). This value is in good agreement with the experimental energy of ≈19 kcal mol^{-1}, measured for FOR derivatives.[5,6] The inverse reaction features an activation energy of 6 kcal mol^{-1}, similarly to what was found in ref 13.

Structural Features. Although the OH^- ion does not relax properly with respect to the minimum of the harmonic restraint, the *structural* features of the direct simulations have reproduced the same ones found in the inverse reaction. Thus, for sake of clarity, we will describe the reaction as the OH^- attack.

The equilibrium distance of the tetrahedral adduct is found at a $C-O_{HYD}$ distance of 1.55 Å. The TS is located at a $C-O_{HYD}$ distance of 2.20 Å, which is considerably longer than the average TS distance of the water addition. The orientation of the hydroxyl ion with respect to the C atom is correlated to the reaction coordinate; in fact, the average value of the angle formed by H_{HYD}, O_{HYD}, and C atoms, as the reactants are further than the TS region, is almost 180°. This geometry is preserved until the $C-O_{HYD}$ distance approaches that of the TS. The reaction occurs as the $H_{HYD}-O_{HYD}-C$ angle bends to a value of about 100°.

The four ligands never leave the solvation shell as the reaction coordinate remains out of the TS region (approximately located between 2.0 and 2.3 Å). The average $O_{HYD}-H$ distance (1.7 ± 0.3 Å) is shorter than H-bonds formed in bulk water (≈1.9 Å). The number of water oxygens H bonded to O_{HYD} decreases from four to three, before the TS (Figure 6b). At the TS, the OH^- reacts when the $H_{HYD}-O_{HYD}-C$ angle bends suitably, due to thermal fluctuations. After the TS, one of the three remaining OH^--bound water molecules is lost (Figure 6d).

The energetics of our calculations are comparable with those calculated by Warshel et al.[2] and Kollman et al.;[11] however, the present study differs for the description of the solvation shell dynamics of the OH^-; indeed, the solvent is implicitly treated in Warshel's calculations,[2] whereas the empirical potential describing the OH^--solvent interaction in ref 11 provides a different geometry for the solvation structure of OH^- (average number of H-bonds of about 5.8).

Electronic Structures. At all the $C-O_{HYD}$ distances, the MD-averaged dipole moment of the four water molecules forming H-bonds with the OH^- anion are appreciably larger than those of bulk water (≈3.2 and 3.0 D, respectively). The polarization of the OH^-, for $C-O_{HYD}$ distances larger than that of the TS, results to be negligible (Figure 8b), suggesting that the long-range interaction between OH^- and FOR does not play any crucial role.

Changes in the electronic structure along the reaction are observed after the TS is crossed (Figure 7b). Thus, the features of the reaction appear to be related to the solvent effects, as opposed to electronic properties. This suggests that the activation free energy for the base-catalyzed reaction is completely solvent induced, as stated in refs 11 and 12.

4. Conclusions

In this paper, we give an energetic and structural description of the first step of formamide hydrolysis in water at physiological and basic pH, by using Car−Parrinello[35] MSMD simulations.[36,62,63]

Hydrolysis of formamide in pure water is extremely unfavored at pH = 7. The activation free energy, calculated for the direct and inverse reactions, is about 44 kcal mol^{-1}. Reaction occurs through a late TS, which leads to a tetrahedral intermediate. This very labile intermediate is characterized by a charge separation, and it is easily deprotonated by solvent water. The water solvation shell scarcely influences the reaction.

The free-energy barrier for the OH^- addition can be calculated only for the reverse reaction, because the relaxation times of the hydroxyl ion solvation shell are much larger than the external perturbation (eq 3) to let its disruption to occur within typical MSMD times. Nevertheless, the present study provides a detailed description of the reaction mechanism. Approaching of the hydroxyl ion to the TS occurs only after the loss of a water molecule in its solvation shell; the water molecules H-bonding to OH^- pass from four to three. The TS is then crossed as fluctuations in the new solvation shell allow the proper geometry between OH^- and FOR to be reached. Although the reaction barrier is solvent induced, as previously proposed,[11] it must be pointed out that these findings might be affected by a choice of the exchange-correlation functional other than BLYP. We stress here anyway that the calculated reaction barrier (≈15 kcal mol^{-1}) is in agreement with experimental data.

In conclusion, the MSMD methodology appears to be a fast and reliable technique to study chemical processes; though, a special care has to be paid when dealing with transformations that require other rearrangements of the system, characterized by short relaxation times. In these cases, standard constraint dynamics,[41,87] although computationally more expensive, may lead to better results.

Particularly powerful is the use of this approach in combination with mixed quantum mechanics/molecular mechanics techniques, which is expected to provide a relatively fast way for the calculation of free-energy activation barriers of enzymatic reactions.[88] Here, preorientation of the reactants in the catalytic pocket should provide optimal conditions for convergence of

free-energy profiles, as a monodimensional approximation of the reaction coordinate is usually satisfactory.[85,86]

Acknowledgment. MURST Cofin is acknowledged for financial support.

References and Notes

(1) Vandeputte-Rutten, L.; Gross, P. *Curr. Opin. Struct. Biol.* **2002**, *12*, 704−708.
(2) Štrajbl, M.; Florián, J.; Warshel, A. *J. Am. Chem. Soc.* **2000**, *122*, 5354−5366.
(3) Hine, J.; King, R. S.-M.; Midden, W. R.; Sinha, A. *J. Org. Chem.* **1981**, *46*, 3186−3189.
(4) Robinson, B. A.; Tester, J. W. *Int. J. Chem. Kinet.* **1990**, *22*, 431−448.
(5) Slebocka-Tilk, H.; Bennet, A. J.; Hogg, H. J.; Brown, R. S. *J. Am. Chem. Soc.* **1991**, *112*, 8507−8514.
(6) Guthrie, J. P. *J. Am. Chem. Soc.* **1974**, *96*, 3608−3615.
(7) Oie, T.; Loew, G. H.; Burt, S. K.; Binkley, J. S.; MacElroy, R. D *J. Am. Chem. Soc.* **1982**, *104*, 6169−6174.
(8) Jensen, J. H.; Baldridge, K. K.; Gordon M. S. *J. Phys. Chem.* **1992**, *96*, 8340−8351.
(9) Kallies, B.; Mitzner, R. J. *J. Mol. Model.* **1998**, *4*, 183−196.
(10) Weiner, S. J.; Singh, U. C.; Kollman, P. A. *J. Am. Chem. Soc.* **1985**, *107*, 2219−2229.
(11) Bakowies, D.; Kollman, P. A. *J. Am. Chem. Soc.* **1999**, *121*, 5712−5726.
(12) Madura, J. D.; Jorgensen, W. L. *J. Am. Chem. Soc.* **1986**, *108*, 2517−2527.
(13) Warshel, A.; Russell, S. T. *J. Am. Chem. Soc.* **1986**, *108*, 6569−6579.
(14) Warshel, A.; Sussman, F.; Hwang, J. K. *J. Mol. Biol.* **1988**, *201*, 139−159.
(15) Scheiner, S.; Kleier, D. A.; Lipscomb, W. N. *Proc. Natl. Acad. Sci. U. S. A.* **1975**, *72*, 2606−2610.
(16) Dewar, M. J. S.; Storch, D. M. *Proc. Natl. Acad. Sci. U. S. A.* **1985**, *82*, 2225−2229.
(17) Taira, K.; Gorenstein, D. G. *Bull. Chem. Soc. Jpn.* **1987**, *60*, 3625.
(18) Daggett, V.; Schröder, S.; Kollman, P. J. *J. Am. Chem. Soc.* **1991**, *113*, 8926−8935.
(19) Krug, J. P.; Popelier, P. L. A.; Bader, R. F. W. *J. Phys. Chem.* **1992**, *96*, 7604.
(20) Harrison, M. J.; Burton, N. A.; Hillier, I. H.; Gould I. R. *Chem. Commun.* **1996**, 2769−2770.
(21) Dive, G.; Dehareng, D.; Peeters, D. *Int. J. Quantum Chem.* **1996**, *58*, 85−107.
(22) Antonczak, S.; Ruiz-Lopez, M.; Rivail, J. L. *J. Mol. Model.* **1997**, *3*, 434−442.
(23) Baeten, A.; Maes, D.; Geerlings, P. *J. Theor. Biol.* **1998**, *195*, 27−40.
(24) Cramer, C. J.; Truhlar, D. G. *Chem. Rev.* **1999**, *99*, 2161−2200.
(25) Tomasi, J.; Persico, M. *Chem. Rev.* **1994**, *94*, 2027.
(26) Florián, J.; Warshel, A. *J. Phys. Chem. B* **1998**, *102*, 719−734.
(27) Florián, J.; Åqvist, J.; Warshel, A. *J. Am. Chem. Soc.* **1998**, *120*, 11524.
(28) Bruni, F.; Ricci, M. A.; Soper, A. K. *J. Chem. Phys.* **2001**, *114*, 8056−8063.
(29) Tuckerman, M. E.; Laasonen, K.; Sprik, M.; Parrinello, M. *J. Phys. Chem.* **1995**, *99*, 5749.
(30) Tuckerman, M. E.; Laasonen, K.; Sprik, M.; Parrinello, M. *J. Chem. Phys.* **1995**, *103*, 150−161.
(31) Tuckerman, M. E.; Marx, D.; Parrinello, M. *Nature* **2002**, *417*, 925−929.
(32) Chen, B.; Park, J. M.; Ivanov, I.; Tabacchi, G.; Klein, M. L.; Parrinello, M. *J. Am. Chem. Soc.* **2002**, *124*, 8534−8535.
(33) Zhu, Z.; Tuckerman, M. E. *J. Phys. Chem. B* **2002**, *106*, 8009−8018.
(34) (a) Librovich, N. B.; Maiorov, V. D. *Russ. J. Phys. Chem.* **1982**, *56*, 380−383. (b) Amo, Y.; Tominaga, Y. *J. Raman Spectrosc.* **2000**, *31*, 547−553.
(35) Car, R.; Parrinello, M. *Phys. Rev. Lett.* **1985**, *55*, 2471−2474.
(36) (a) Jarzynski, C. *Phys. Rev. Lett.* **1997**, *78*, 2690−2693. (b) Jarzynski, C. *Phys. Rev. E* **1997**, *56*, 5018−5035.
(37) Laio, A.; Parrinello, M. *Proc. Natl. Acad. Sci. U. S. A.* **2002**, *99*, 12562−12566.
(38) Passerone, D.; Parrinello, M. *Phys. Rev. Lett.* **2001**, *87*, 108302−108305.
(39) Elber, R. *Recent developments in theoretical studies of proteins*; World Scientific: Singapore, 1996.
(40) Dellago, C.; Bolhuis, P. G.; Chandler, D. *J. Chem. Phys.* **1999**, *110*, 6617−6624.
(41) Sprik, M.; Ciccotti, G. *J. Chem. Phys.* **1998**, *109*, 7737−7744.
(42) Vandevondele, J.; Rothlisberger, U. *J. Am. Chem. Soc.* **2002**, *124*, 8163−8171.
(43) For example: Perkins, T. T.; Smith, D. E.; Chu, S. *Science* **1994**, *264*, 819−822.
(44) Florin, E. L.; Moy, V. T.; Gaub, H. E. *Science* **1994**, *264*, 415−417.
(45) Strick, T. R.; Allemand, J. F.; Bensimon, D.; Bensimon, A.; Croquette, V. *Science* **1996**, *271*, 1835−1837.
(46) Smith, S. B.; Cui, Y. J.; Bustamante, C. *Science* **1996**, *271*, 795−799.
(47) Tskhovrebova, L.; Trinick, J.; Sleep, J. A.; Simmons, R. M. *Nature* **1997**, *387*, 308−312.
(48) Rief, M.; Gautel, M.; Oesterhelt, F.; Fernandez, J. M.; Gaub H. E. *Science* **1997**, *276*, 1109−1112.
(49) Oberhauser, A. F.; Marszalek, P. E.; Erickson, H. P.; Fernandez, J. M. *Nature* **1998**, *393*, 181−185.
(50) Oesterhelt, F.; Oesterhelt, D.; Pfeiffer, M.; Engel, A.; Gaub, H. E.; Müller, D. J. *Science* **2000**, *288*, 143−146.
(51) Merkel, R.; Nassoy, P.; Leung, A.; Ritchie, K.; Evans, E. *Nature* **1999**, *397*, 50−53.
(52) Kellermayer, M. S. Z.; Smith, S. B.; Granzier, H. L.; Bustamante, C. *Science* **1997**, *276*, 1112−1116.
(53) Isralewitz, B.; Izrailev, S.; Schulten, K. *Biophys. J.* **1997**, *73*, 2972−2979.
(54) Marszalek, P. E.; Lu, H.; Li, H.; Carrion-Vazquez, M.; Oberhauser, A. F.; Schulten, K.; Fernandez, J. M. *Nature* **1999**, *402*, 100−103.
(55) Paci, E.; Karplus, M. *J. Mol. Biol.* **1999**, *288*, 441−459.
(56) Hendrix, D. A.; Jarzynski, C. *J. Chem. Phys.* **2001**, *114*, 5974−4981.
(57) Hummer, G. *J. Chem. Phys.* **2001**, *114*, 7330−7337.
(58) Jensen, M. Ø.; Park, S.; Tajkhorshid, E.; Schulten, K. *Proc. Natl. Acad. Sci. U. S. A.* **2002**, *99*, 6731−6736.
(59) Cascella, M.; Guidoni, L.; Rothlisberger, U.; Maritan, A.; Carloni, P. *J. Phys. Chem. B* **2002**, *106*, 13027−13032.
(60) Vidossich, P.; Cascella, M.; Carloni, P. *Proteins*, in press.
(61) Liphardt, J.; Dumont, S.; Smith, S. B.; Tinoco, I.; Bustamante, C. *Science* **2002**, *296*, 1832−1835.
(62) Crooks, G. E. *Phys. Rev. E* **2000**, *61*, 2361−2366.
(63) Hummer, G.; Szabo, A. *Proc. Natl. Acad. Sci. U. S. A.* **2001**, *98*, 3658−3661.
(64) (a) Rugei, S.; Klein, M. L. *J. Am. Chem. Soc.* **2001**, *113*, 9484−9485. (b) Raugei, S.; Klein, M. L. *J. Chem. Phys.* **2002**, *116*, 196−202.
(65) Hutter, J.; Alavi, A.; Deutsch, T.; Bernasconi. M.; Goedecker, St.; Marx, D.; Tuckerman, M. E.; Parrinello, M. *CPMD*; MPI für Festkörperforschung and IBM Research Laboratory: Stuttgart and Zürich, 1995−2001; version 3.5.
(66) Becke, A. D. *Phys. Rev. A* **1988**, *38*, 3098−3100.
(67) Lee, C.; Yang, W.; Parr, R. G. *Phys. Rev. B* **1988**, *37*, 785−789.
(68) Troullier, N.; Martins, J. L. *Phys. Rev. B* **1991**, *43*, 1943−2006.
(69) Laasonen, K.; Sprik, M.; Parrinello, M.; Car, R. *J. Phys. Chem.* **1993**, *99*, 9080−9089.
(70) Silvestrelli, P. L.; Marzari, N.; Vanderbilt, D.; Parrinello, M. *Solid State Commun.* **1998**, *107*, 7−11.
(71) Marzari, N.; Vanderbilt, D. *Phys. Rev. B* **1997**, *56*, 12847−12865.
(72) Alber, F.; Folkers, G.; Carloni, P. *J. Phys. Chem.* **1999**, *103*, 6121−6126.
(73) Nose', S. J. *J. Chem. Phys.* **1984**, *81*, 511−519.
(74) Hoover, W. G. *Phys. Rev. A* **1985**, *31*, 1695−1697.
(75) Martyna, G.; Tuckerman, M.; Klein, M. L. *J. Chem. Phys.* **1992**, *97*, 2635.
(76) Sprik, M. *Chem. Phys.* **2000**, *258*, 139−150.
(77) Baker, J.; Andzelm, J.; Muir M.; Taylor, P. R. *Chem. Phys. Lett.* **1995**, *237*, 53−60.
(78) Parthiban, S.; de Oliveira, G.; Martin, J. M. L. *J. Phys. Chem. A* **2001**, *105*, 895−904.
(79) Jorgensen, W. L.; Swenson, J. *J. Am. Chem. Soc.* **1985**, *107*, 1489.
(80) (a) Craw, J. S.; Guest, J. M.; Cooper, M. D.; Burton, N. A.; Hillier, I. H. *J. Phys. Chem.* **1996**, *100*, 6304. (b) Chalmet, S.; Ruiz-Lopez, M. F. *J. Chem. Phys.* **1999**, *111*, 1117−1125.
(81) Sprik, M.; Klein, M. L.; Watanabe, K. *J. Phys. Chem.* **1990**, *94*, 6483−6488.
(82) Smith, D. E.; Dang, L. X. *J. Chem Phys.* **1994**, *100*, 3757−3766.
(83) Kropman, M. F.; Bakker, H. J. *Science* **2001**, *291*, 2118−2120.
(84) Piana, S.; Bucher, D.; Carloni, P.; Rothlisberger, U. Reaction Mechanism of HIV-1 Protease by hybrid Car−Parrinello/Classical MD simulations. Submitted.
(85) Sulpizi, M.; Laio, A.; Vandevondele, J.; Cattaneo, A.; Rothlisberger, U.; Carloni, P. *Proteins* **2003**, *52*, 212−224.
(86) Piana, S.; Carloni, P.; Parrinello, M. *J. Mol. Biol.* **2002**, *319*, 567−583.
(87) Carter, E. A.; Ciccotti, G.; Hynes, J. T.; Kapral, R. *Chem. Phys. Lett.* **1989**, *156*, 472−477.
(88) Carloni, P.; Rothlisberger, U.; Parrinello, M. *Acc. Chem. Res.* **2002**, *35*, 455−464.